

hep-th/0612143
PUPT-2219

Jet-quenching and momentum correlators from the gauge-string duality

Steven S. Gubser

Joseph Henry Laboratories, Princeton University, Princeton, NJ 08544

Abstract

I relate the jet-quenching parameter, as defined by $\hat{q} = p_\perp^2/\lambda$, for an external quark moving through a thermal plasma of $\mathcal{N} = 4$ gauge theory, to a two-point function of transverse displacements of the quark's worldline. This two-point function can be computed using the gauge-string duality. I comment on the possible relevance of the string theory calculation to heavy quarks propagating through a quark-gluon plasma.

1 Introduction

An important parameter for describing the radiative energy loss of hard partons propagating through the quark-gluon plasma (QGP) produced at the Relativistic Heavy Ion Collider (RHIC) is the BDMPS [1] transport coefficient, or jet-quenching parameter, $\hat{q} = p_\perp^2/\lambda$. Here p_\perp is the transverse momentum imparted to the parton after it has traveled a distance λ through the medium. Recently, a proposal has been made [2] for extracting \hat{q} for $\mathcal{N} = 4$ gauge theory from a Wilson loop calculation amenable to solution through techniques of classical string theory.¹ Independently, proposals have been made [3, 4, 5] for describing the energy loss from heavy quarks also in terms of classical string configurations. Earlier work in a somewhat similar spirit includes [6], and subsequent work includes extensions to non-conformal theories [7, 8, 9, 10], non-zero chemical potentials [11, 12, 13, 14, 15, 16], and other deformations of $\mathcal{N} = 4$ gauge theory [17]; studies of directional emission [18, 19] and the relation to the magnetic string tension [20]; and calculations of drag on particles carrying higher representations of the gauge group [21].

The venue for the string theory calculations is the gauge-string duality [22, 23, 24] (for reviews see [25, 26, 27]), in particular the computation of Wilson loops through a dual classical configuration of fundamental strings in anti-de Sitter space, as first considered in [28, 29].

The aim of the present paper is to consider an alternate route from classical string configurations to the jet-quenching parameter to the one presented in [2]. The defining equation $\hat{q} = p_\perp^2/\lambda$ will be compared to a two-point function extracted from a slight elaboration of the recipe of [30], which itself is a variant of the usual AdS/CFT prescription for Green's functions [23, 24]. The central result is that, for $\mathcal{N} = 4$ gauge theory at large N and strong 't Hooft coupling, and for v close to 1,

$$\hat{q} \approx 2\pi\sqrt{g_{YM}^2 N} \frac{v}{\sqrt{1-v^2}} T^3, \quad (1)$$

where v is the velocity of the heavy quark relative to the medium. The right hand side of (1) is the relativistic, low-frequency limit of a more general expression which I will show how to evaluate (numerically) for arbitrary velocity and frequency. This more general expression gives values of \hat{q} which are bounded below by (1).

Whereas the authors of [2] argue that their method can be applied to light quarks, the

¹Note that the operational definition of \hat{q} in [2] is not $\hat{q} = p_\perp^2/\lambda$, but instead refers to a partially light-like Wilson loop.

configurations considered in this paper are unmistakably associated with external quarks—formally, an infinitely massive point-like color source in the fundamental representation. So comparisons with heavy partons propagating through a real-world QGP are best justified for quarks whose mass is well above the temperature of the QGP. Charm and bottom quarks are the natural candidates in the context of RHIC physics.

The organization of the rest of this paper is as follows. In section 2 I give a simple-minded account of the diffusion of transverse momentum in terms of Langevin dynamics. The purpose of this account is to focus attention on the two-point function of the stochastic transverse force, whose evaluation in string theory is the goal of sections 3, 4, and 5. The reader wishing to skip to the answer may refer to (34) for the definition of a dimensionless form \hat{Q} of the jet-quenching parameter whose dependence on v and a dimensionless form of the frequency, $\Omega = \omega/\pi T$, is summarized in figure 2. In section 6 I attempt to make predictions about the jet-quenching parameter for heavy quarks in QCD. This discussion suffers from the usual difficulties of relating two significantly different theories, namely $\mathcal{N} = 4$ super-Yang-Mills and QCD. Appendix A contains an exposition of the causal structure of the trailing string worldsheet. Appendix B presents some estimates of the speed above which trailing string calculations may become unreliable.

2 Langevin dynamics and momentum correlators

A simple account of the linear growth of p_\perp^2 with path length can be given in terms of Langevin dynamics. Consider a random force $F_i(t)$ acting on the transverse momentum of a parton:

$$\frac{dp_i}{dt} = F_i(t) \quad \langle F_i(t_1)F_j(t_2) \rangle = K_{ij}(t_1 - t_2), \quad (2)$$

where $K_{ij}(t)$ is an integrable 2×2 matrix-valued function. If one assumes $p_\perp(0) = 0$, then at sufficiently late times t (meaning times larger than the characteristic time-scales of $K_{ij}(t)$) one has

$$\langle p_\perp(t)^2 \rangle = \delta^{ij} \langle p_i(t)p_j(t) \rangle = \int_0^t dt_1 \int_0^t dt_2 \delta^{ij} K_{ij}(t_1 - t_2) \approx \kappa t, \quad (3)$$

where by definition

$$\kappa = \int_{-\infty}^{\infty} dt \delta^{ij} K_{ij}(t). \quad (4)$$

Comparing with $\hat{q} = p_\perp^2/\lambda$, one extracts

$$\hat{q} = \frac{\kappa}{v}. \quad (5)$$

One may pass to frequency space by defining

$$p(t) = \int_{-\infty}^{\infty} \frac{d\omega}{2\pi} e^{-i\omega t} p(\omega) \quad K_{ij}(t) = \int_{-\infty}^{\infty} \frac{d\omega}{2\pi} e^{-i\omega t} K_{ij}(\omega). \quad (6)$$

Then (2) may be rephrased as

$$\langle p_i(\omega_1) p_j(\omega_2) \rangle = -\frac{2\pi\delta(\omega_1 + \omega_2)}{\omega_1\omega_2} K_{ij}(\omega_1) \quad \kappa = \delta^{ij} K_{ij}(0), \quad (7)$$

where the last expression refers to the Fourier transform $K_{ij}(\omega)$ at $\omega = 0$.

A brief statement of the aim of the next three sections is to extract $K_{ij}(\omega)$ for external quarks propagating through a thermal state of $\mathcal{N} = 4$ gauge theory, using the gauge-string duality.

3 Transverse oscillations of the trailing string

A thermal state of strongly coupled $\mathcal{N} = 4$ gauge theory is encoded in the near-extremal D3-brane background [31], of which the relevant part for this analysis is the AdS_5 -Schwarzschild geometry,

$$ds^2 = G_{\mu\nu} dx^\mu dx^\nu = \frac{L^2}{z^2} \left(-h dt^2 + d\bar{x}^2 + \frac{dz^2}{h} \right) \quad h = 1 - \frac{z^4}{z_H^4} \quad z_H = \frac{1}{\pi T}, \quad (8)$$

where T is the Hawking temperature of the horizon at $z = z_H$. I will generally prefer to use a rescaled radial coordinate $y = z/z_H$. The action for a classical string propagating in AdS_5 -Schwarzschild is

$$S = -\frac{1}{2\pi\alpha'} \int d^2\sigma \sqrt{-\det g_{\alpha\beta}} \quad g_{\alpha\beta} = G_{\mu\nu} \partial_\alpha X^\mu \partial_\beta X^\nu. \quad (9)$$

The trailing string of [3, 5] can be described in static gauge, $\sigma^\alpha = (t, y)$, as

$$x^1 = vt + \xi(y) \quad \xi(y) = \frac{ivz_H}{4} \left(\log \frac{1-iy}{1+iy} + i \log \frac{1+y}{1-y} \right), \quad (10)$$

with $x^2 = x^3 = 0$. Consider now fluctuations in the x^2 direction. To ease notation, set $x^2 = \phi$. Expanding (9) to quadratic order leads to an action

$$S_2 = - \int dt dy \frac{1}{2} \partial_\alpha \phi \mathcal{G}^{\alpha\beta} \partial_\beta \phi \quad \mathcal{G}^{\alpha\beta} = \frac{L^2/2\pi\alpha'}{y_S^2 z_H^2} \begin{pmatrix} -\frac{1-y^4 y_S^4}{y^2(1-y^4)^2} z_H & -\frac{v^2}{1-y^4} \\ -\frac{v^2}{1-y^4} & \frac{y_S^4-y^4}{y^2 z_H} \end{pmatrix}, \quad (11)$$

where I have defined

$$y_S = (1-v^2)^{1/4}. \quad (12)$$

The equation of motion following from (11) is

$$\partial_\alpha J_S^\alpha = 0 \quad J_S^\alpha = \mathcal{G}^{\alpha\beta} \partial_\beta \phi. \quad (13)$$

J_S^α is the Noether current associated with additive shifts of ϕ . It is the worldsheet current of spacetime momentum in the x^2 direction [32].

The general solution of interest can be represented as

$$\phi(t, y) = \int_{-\infty}^{\infty} \frac{d\omega}{2\pi} \phi_0(\omega) \Psi(\omega, t, y) \quad \Psi(\omega, t, y) = e^{-i\omega t} \psi(\omega, y). \quad (14)$$

The wave-functions $\Psi(\omega, t, y)$ satisfy several conditions which will be built up step by step and then summarized at the end of this section. First, its radial factor $\psi(\omega, y)$ satisfies the following equation (derived from the equation of motion for ϕ):

$$[s(\omega, y) \partial_y^2 + t(\omega, y) \partial_y + u(\omega, y)] \psi(\omega, y) = 0, \quad (15)$$

where

$$\begin{aligned} s(y) &= -y(1-y^4)^2(y_S^4-y^4) \\ t(\omega, y) &= 2(1-y^4) [1-y^8-v^2(1-y^4+iy^3 z_H \omega)] \\ u(\omega, y) &= -yz_H \omega [(1-y^4)z_H \omega + v^2 y^4 (4iy + z_H \omega)]. \end{aligned} \quad (16)$$

The radial equation (15) has regular singular points at the zeroes of $s(y)$: $y = 0$, $y = \varkappa$, and $y = \varkappa y_S$ where \varkappa is any fourth root of unity. The most interesting of these is $y = y_S$, corresponding to some intermediate point on the string. What is special about this point is that it is the location of a horizon of the induced metric on the worldsheet. An intuitive way to see this is that a point on the trailing string with y held fixed follows a timelike trajectory if $y < y_S$ and a spacelike one if $y > y_S$.² So the region $y < y_S$ corresponds to the exterior of

²A closely related observation [3, 33, 34, 35] is that there are no-drag configurations of mesons represented

the “black hole on the worldsheet,” and $y > y_S$ corresponds to the interior. No signal from the interior can propagate classically to the exterior. Instead, signals in the interior region must by causality travel down the string. But there should be some Hawking radiation from the worldsheet horizon upward toward $y = 0$, and it is natural to suppose that it relates to the jet-quenching parameter \hat{q} . I will not make this connection directly, but the two-point function that I will compute is related to both classical absorption and spontaneous emission by the worldsheet horizon.

Although (15) does not seem to be explicitly solvable, certain limits of it are tractable. For example, to leading order in small y one finds

$$\psi(\omega, y) = 1 + C^\infty(\omega)y^3, \quad (17)$$

up to an overall factor which I set to unity as part of the conditions on $\Psi(\omega, t, y)$. Near the worldsheet horizon, to leading order in small $y_S - y$, one finds

$$\psi(\omega, y) = C_-^H(\omega) + C_+^H(\omega)(y_S - y)^{i\omega z_H/2y_S}. \quad (18)$$

For $\omega > 0$, the solution in (18) with coefficient C_+^H clearly corresponds to an outgoing wave, because the phase increases as one goes to smaller values of y . The standard horizon boundary condition, then, is $C_+^H = 0$. To justify this statement completely, one should show that $C_+^H = 0$ amounts to stipulating that $\Psi(\omega, t, y)$ should depend only on the infalling coordinate at the horizon. To leading order close to the horizon, the infalling and outgoing coordinates are

$$u_- = t \quad u_+ = t - \frac{z_H}{2y_S} \log(y_S - y). \quad (19)$$

A justification of (19), together with a more complete analysis of the induced metric on the worldsheet, is postponed to appendix A.

Let us now review the properties of the wave-functions $\Psi(\omega, t, y)$:

1. $\Psi(\omega, t, y)$ is a solution of the wave equation for ϕ .
2. $\Psi(\omega, t, 0) = e^{-i\omega t}$.
3. $\Psi(\omega, t, y)$ is independent of y near the horizon, corresponding to an infalling wave.
4. $\Psi(\omega, t, y)^* = \Psi(-\omega, t, y)$. To see this, note that complex conjugation is equivalent to

as strings with both ends attached to branes in AdS_5 -Schwarzschild provided the string between the quarks hangs no lower than $y = y_S$.

sending $\omega \rightarrow -\omega$ in the radial equation (15), and that the boundary condition at the horizon is preserved by complex conjugation. This property guarantees that $\phi(t, y)$ is real everywhere provided $\phi_0(\omega)^* = \phi_0(-\omega)$.

4 Momentum correlators from the trailing string

The retarded Green's function of the operator \mathcal{O} dual to ϕ is

$$G_R(\omega) \equiv -i \int_{-\infty}^{\infty} dt e^{i\omega t} \theta(t) \langle [\mathcal{O}(t), \mathcal{O}(0)] \rangle. \quad (20)$$

The proposal for extracting this Green's function from the wave-functions $\Psi(\omega, t, y)$ is

$$G_R(\omega) = -\Psi^*(\omega, t, y) \mathcal{G}^{y\beta} \partial_{\beta} \Psi(\omega, t, y) \Big|_{y=0} = -\mathcal{G}^{y\beta} \partial_{\beta} \log \Psi(\omega, t, y) \Big|_{y=0}, \quad (21)$$

where the notation $|_{y=0}$ means to evaluate at $y = 0$ after taking the derivatives. The difference between (21) and (3.15) of [30] is the use of Ψ rather than ψ .³ Using ψ would amount to restricting the sum over β to $\beta = y$, and this does not make sense in light of worldsheet reparametrization invariance. The expressions in (21) are proportional to the momentum current J_S^{α} associated with $\Psi(\omega, t, y)$, dotted into the normal form dy at the boundary. Also, if the number current associated with $\Psi(\omega, t, y)$ is defined as

$$J^{\alpha} = \frac{1}{2i} \mathcal{G}^{\alpha\beta} \Psi^* \overleftrightarrow{\partial}_{\beta} \Psi, \quad (22)$$

then

$$\text{Im } G_R(\omega) = -J^y, \quad (23)$$

and because J^{α} is conserved, the right hand side of (23) can be evaluated at any y . The number flux is positive at the horizon for $\omega > 0$ as a consequence of the infalling boundary conditions, so one finds from (23) that

$$\text{Im } G_R(\omega) < 0 \quad \text{for } \omega > 0. \quad (24)$$

This is the correct sign to describe dissipative dynamics. Again, if ψ had been used instead of Ψ , the connection with the conserved number current would be broken. In [30] a restriction

³Actually there seems to be one further difference: an overall sign. Possibly I have misunderstood the notation used [30]. Anyway, I claim that the sign in (21) is the right one.

was made to consider only diagonal metrics, so the question of including dependence of the wave-function on coordinates other than the radial one never arose. (The context was slightly different: instead of $\mathcal{G}^{\alpha\beta}$, the metric of interest was the line element of the bulk spacetime.) But (21) is clearly in the spirit of [30] and its antecedent [23]: note for instance the similarity with (27) of [23].

Just as in the examples treated in [30], the real part of (21) may be recovered using a more conventional AdS/CFT formulation in which the quadratic string theory action is the generating functional for the two-point function. But it turns out that the imaginary part will be of greater interest, due to its connection with the dissipative dynamics. More specifically, again following [30], consider the symmetrized Wightman function

$$G(\omega) \equiv \frac{1}{2} \int_{-\infty}^{\infty} dt e^{i\omega t} \langle \mathcal{O}(t) \mathcal{O}(0) + \mathcal{O}(0) \mathcal{O}(t) \rangle = -\coth \frac{\omega}{2T} \text{Im } G_R(\omega). \quad (25)$$

Briefly, the claim is that $G(\omega) = K_{22}(0)$, so $\kappa = 2G(0)$. This follows if $\mathcal{O}(t)$ is identified with $\pm \dot{p}_2(t)$.

Here is a somewhat informal argument for identifying $\mathcal{O}(t)$ with $-\dot{p}_2(t)$, i.e. minus the force exerted in the x^2 direction. Consider the action

$$S_q[\phi(t)] = \int dt L(\dot{\phi}_0) \quad (26)$$

for an external quark propagating through the thermal medium along a path

$$x^1(t) = vt \quad x^2(t) = \phi_0(t). \quad (27)$$

I have excluded explicit dependence on ϕ_0 (and t) from L because the medium is assumed to be translationally invariant. Note that this does not imply conservation of transverse momentum: S_q is evaluated under the path integral and includes couplings to the gauge theory. For small deviations ϕ_0 from a straight path,

$$S_q \approx \int dt \dot{\phi}_0 \frac{\partial L}{\partial \dot{\phi}_0} = \int dt \dot{\phi}_0 p_\phi = - \int dt \phi_0 \dot{p}_\phi. \quad (28)$$

Of course, $p_\phi = p_2$. Altogether, the generating functional for the two-point functions of interest is

$$Z[\phi_0] = \left\langle \exp \left\{ -i \int dt \phi_0 \dot{p}_2 \right\} \right\rangle, \quad (29)$$

whence the conclusion $\mathcal{O} = -\dot{p}_2$. More formally, $p_2(t)$ should be regarded as the operator

which generates a local displacement at time t of the path of the Wilson loop for the external quark.

The Green's functions of interest can conveniently be expressed in terms of the quantities

$$X = \frac{2v^2\omega z_H}{3(1-v^2)} \quad Y = \frac{3\sqrt{1-v^2}}{4\pi z_H^3} \frac{L^2}{\alpha'} = \frac{3\sqrt{g_{YM}^2 N}}{4\pi z_H^3} \sqrt{1-v^2} \quad (30)$$

together with C^∞ : a short calculation starting from (17), (21), and (25) yields

$$G_R(\omega) = -Y(2C^\infty + iX) \quad G(\omega) = Y \coth \frac{\omega}{2T} (2 \operatorname{Im} C^\infty + X). \quad (31)$$

Comparing with (25) with (2) and the first equation in (7), and recalling that $\mathcal{O}(t) = -\dot{p}_2(t)$, one arrives at

$$K_{ij}(\omega) = \delta_{ij}G(\omega). \quad (32)$$

Referring to (5) and the second equation in (7), it is natural to define a frequency-dependent jet-quenching parameter

$$\hat{q}(\omega) = \frac{2}{v}G(\omega). \quad (33)$$

Then $\hat{q}(0) = p_\perp^2/\lambda$ quantifies transverse momentum diffusion in the limit of large path length λ .

All expressions can be rendered dimensionless by introducing factors of the temperature. Let's define

$$\Omega \equiv \omega z_H = \frac{\omega}{\pi T} \quad \hat{Q}(\Omega, v) \equiv \frac{1}{2\pi\sqrt{g_{YM}^2 N}} \frac{\hat{q}(\omega)}{T^3}. \quad (34)$$

The notation $\hat{Q}(\Omega, v)$ emphasizes that \hat{Q} is a function only of the dimensionless quantities Ω and v . (This is a consequence of conformal invariance.) Unraveling the various definitions, one finds

$$\hat{Q}(\Omega, v) = \frac{v}{\sqrt{1-v^2}} \left(1 + \frac{2 \operatorname{Im} C^\infty}{X} \right) \frac{\pi\Omega}{2} \coth \frac{\pi\Omega}{2}. \quad (35)$$

The factor in parentheses depends on both v and Ω , and it must be determined through a numerical integration of the radial equation (15) for transverse oscillations of the string.

5 Numerical results

The differential equation (15) depends on ω and z_H only through the combination $\Omega = \omega z_H$. The only other quantity one must specify in order to carry out a numerical integration is v ,

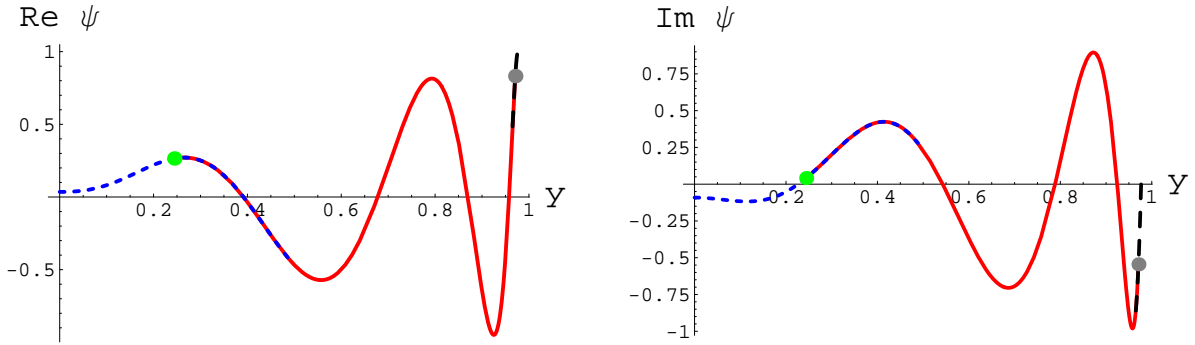


Figure 1: Matching series onto a numerical solution of (15) with $v = 0.3$ and $\Omega = 10$. This is a relatively difficult set of parameters because the radius of convergence of the near-horizon solution is small, but it is clear that the match to numerics is very good. The numerical integration (solid red curve) was seeded with initial conditions from the near-horizon series solution (dashed black curve) at $y = y_i$, shown as the grey point in each plot. The near-boundary series solution (dotted blue curve) was obtained using Wronskian matching conditions at $y = y_f$, shown as the green point in each plot.

because $y_S = (1 - v^2)^{1/4}$. The strategy for finding $\psi(y)$ is to make series expansions around both $y = y_S$ and $y = 0$ and interpolate between them with a direct numerical integration of (15) using Mathematica’s `NDSolve`. The horizon boundary conditions determine $\psi(y)$ up to the overall constant factor C_-^H , so it is natural to seed `NDSolve` with Cauchy data at some point y_i close to y_S and then extract coefficients for the two possible far-field solutions by computing Wronskians at some point y_f close to 0. Choosing y_i and y_f to be much closer to y_S and 0, respectively, than the closest singular points ensures that the series expansions converge quickly. This convergence is better when Ω is small, because in general higher order terms are suppressed by powers of Ω . Overall, the numerical problem is not very difficult, and based on diagnostic plots such as figure 1 I expect that the evaluations of $\hat{Q}(\Omega, v)$ are good to the tenth of a percent level at least out to $\Omega = 10$ and for $v > 0.3$. For lower values of v , y_S is quite close to the actual black hole horizon at $y = 1$, so the convergence properties of the near-horizon solution (at least as I have formulated the series expansion) become worse and worse. But for small v , it is probably better to think about diffusion in all three directions of momentum rather than just transverse, and an analysis along the lines of [4] can be applied.

Summary views of the function $\hat{Q}(\Omega, v)$ are shown in figure 2. The overall behavior in

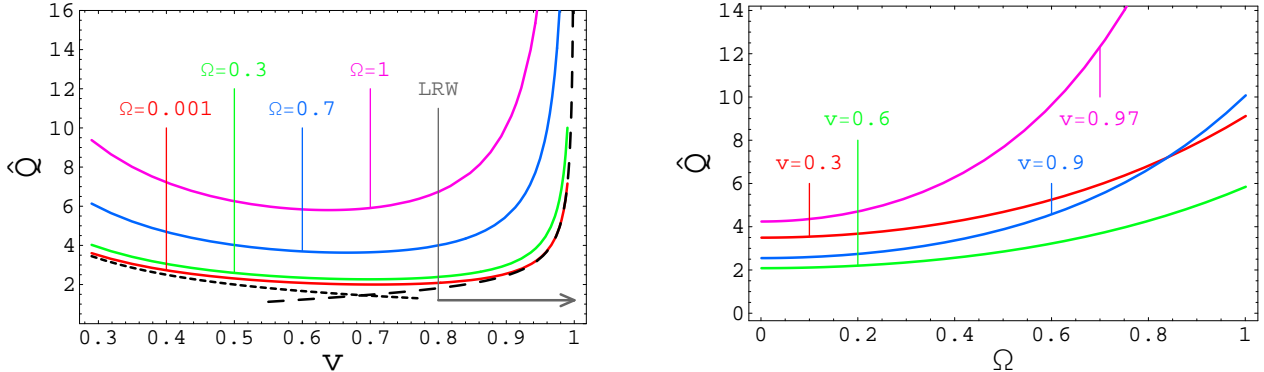


Figure 2: Plots of $\hat{Q}(\Omega, v)$ for fixed Ω (left) and fixed v (right). The dashed and dotted curves are analytic approximations in the limits $\Omega \rightarrow 0$, $v \rightarrow 1$ and $\Omega \rightarrow 0$, $v \rightarrow 0$, respectively: see (36). The horizontal grey arrow shows the value $\hat{Q} \approx 1.2$ corresponding to the result of [2], which is evaluated in a light-like limit, $v = 1$. See the discussion around (47).

the $\Omega \rightarrow 0$ limit can be understood qualitatively from two even simpler limits:

$$\begin{aligned}\hat{Q} &\approx \frac{v(2 - v^2)}{\sqrt{1 - v^2}} && \text{for } \Omega \rightarrow 0 \text{ and } v \text{ close to 1.} \\ \hat{Q} &\approx \frac{1}{v} && \text{for } \Omega \rightarrow 0 \text{ and } v \ll 1.\end{aligned}\tag{36}$$

The leading behavior as $v \rightarrow 1$, $\hat{Q} \approx v/\sqrt{1 - v^2}$, follows from dropping the second term in parentheses from (35). Equivalently, this comes from dropping the $\beta = y$ term in (21). The non-relativistic expression in (36) comes from comparing (34) to (1.13) of [3], which follows more or less directly from the diffusion analysis discussed in both [3] and [4].⁴

Preliminary numerical work suggests that $\hat{Q}(0, v) = 1/v\sqrt{1 - v^2}$ may be the exact $\Omega \rightarrow 0$ expression for all v . Certainly the $\Omega = 0.001$ curve in the left pane of figure 2 is indistinguishable from this analytic form. In section 6 I will make numerical estimates for \hat{q} using the less accurate expression $\hat{Q}(0, v) \approx v/\sqrt{1 - v^2}$. The reason for doing so is that this formula can be derived with no recourse to non-trivial analytic or numerical calculations if one only assumes $|\text{Im } C^\infty| \ll X$ in (35). All numerical estimates will be made for v close enough to 1 that the difference between $v/\sqrt{1 - v^2}$ and $1/v\sqrt{1 - v^2}$ is at the percent level.

The large Ω limit, though perhaps not very relevant for RHIC phenomenology, is interesting because it can be expected to lead to a power law form for the symmetrized Wightman function $G(\omega)$. This expectation is sensible because, far enough above the scale set by the temperature, conformal symmetry permits no other scaling (except powers times logs in spe-

⁴I thank C. Herzog for suggesting this comparison.

cial cases). Because of the identification $\mathcal{O}(t) = -\dot{p}_2(t)$, which is an operator of dimension 2, the expectation is that $G(t) \propto 1/t^4$ for small but non-zero t . In order to continue working with dimensionless quantities, I will express results in terms of

$$\tau = t/z_H \quad \hat{Q}(\tau, v) \equiv \int_{-\infty}^{\infty} \frac{d\Omega}{2\pi} e^{-i\Omega\tau} \hat{Q}(\Omega, v). \quad (37)$$

Expanding the integral

$$\int_{-\infty}^{\infty} d\tau \frac{e^{i\Omega\tau}}{|\tau|^{2\Delta}} = \int_{-\infty}^{\infty} d\tau \frac{2 \cos \Omega\tau}{\tau^{2\Delta}} = \frac{(i\Omega)^{2\Delta} - (-i\Omega)^{2\Delta}}{i\Omega} \Gamma(1 - 2\Delta) \quad (38)$$

around $\Delta = 2$ gives

$$\int_{-\infty}^{\infty} d\tau \frac{e^{i\Omega\tau}}{|\tau|^4} = \frac{\pi}{6} |\Omega|^3 + (\text{analytic in } \Omega). \quad (39)$$

There is an analytic continuation implicit in the result (39): the integral (38) can be evaluated for $\Omega > 0$ and $0 < \Delta < 1/2$ with no regularization, but the integral in (39) is of course highly divergent. Regularization schemes differ in how they prescribe the analytic terms on the right hand side of (39), corresponding to contact terms in real time, supported at $\tau = 0$. Thus a scaling form

$$\hat{Q}(\tau, v) = \frac{\hat{Q}_{\text{scaling}}(v)}{|\tau|^4} + (\text{contact terms}) \quad (40)$$

at small τ corresponds to

$$\hat{Q}(\Omega, v) = \frac{\pi}{6} \hat{Q}_{\text{scaling}}(v) |\Omega|^3 + \hat{Q}_2(v) \Omega^2 + \hat{Q}_0(v) + o(1), \quad (41)$$

where $o(1)$ means tending to 0 as $\Omega \rightarrow \infty$. Note that $\hat{Q}_0(v)$ is not the jet-quenching parameter at zero frequency: the latter is a quantity defined in the infrared, whereas (41) refers to an ultraviolet limit.

For fixed values of v in the range $0.3 < v < 0.98$, the three-parameter ansatz (41) is an excellent fit to numerical evaluations of $\hat{Q}(\Omega, v)$ for $4 \lesssim \Omega \lesssim 20$. I have not attempted to go to higher Ω because I am not sure that the numerical methods being used can be pushed that far. It turns out that

$$\hat{Q}_{\text{scaling}}(v) = \frac{3}{\sqrt{1 - v^2}} \hat{Q}(0, v) \quad (42)$$

to tenth of a percent accuracy. This intriguing result, relating ultraviolet and infrared limits, hints that an entirely analytic treatment might be possible.

6 Discussion

With a string theory prediction of \hat{q} for heavy quarks in hand, one should aim to make predictions of the nuclear modification factor R_{AA} and compare with data, as released most recently by STAR and PHENIX in [36, 37]. I will not get that far for two main reasons: first, the relation between \hat{q} and R_{AA} is not simple; and second, $\mathcal{N} = 4$ super-Yang-Mills and QCD are different enough that it's not entirely clear how to make a crisp prediction for one based on the other. In section 6.1 I will summarize two schemes for comparing $\mathcal{N} = 4$ and QCD, make some numerical estimates of \hat{q} , and comment on qualitative comparisons with other works and with data. In section 6.2 I will consider the relation of \hat{q} to energy loss, which is parametrically different in the trailing string description from the usual relation $dE/dx \propto \hat{q}\lambda$ as found, for example, in [1].

6.1 Numerical estimates of \hat{q}

Referring to (34) and (36), one sees that for high-momentum heavy quarks traversing a thickness $\lambda \gg 1/T$ of $\mathcal{N} = 4$ thermal plasma (so that $\Omega \ll 1$), the AdS/CFT prediction for \hat{q} is⁵

$$\hat{q} \approx 2\pi\sqrt{g_{YM}^2 N} \frac{v}{\sqrt{1-v^2}} T^3. \quad (43)$$

There is considerable uncertainty in how one should translate this result into a prediction for QCD. To characterize this uncertainty, consider the following two comparison schemes:

- An “obvious” comparison scheme is to equate the temperature and the Yang-Mills coupling. I will assume $T = 250$ MeV and $\alpha_s = 0.5$, which are in a representative range for RHIC physics. To summarize:

$$\text{“obvious” scheme:} \quad T_{\mathcal{N}=4} = T_{\text{QCD}} = 250 \text{ MeV} \quad g_{YM}^2 N = 12\pi\alpha_s = 6\pi. \quad (44)$$

- An “alternative” comparison scheme was proposed in [38]. The first part of this prescription is to equate energy density instead of temperature. Thus in any formula (for example (65)) in $\mathcal{N} = 4$ in which T enters, one eliminates it in favor of a power of the energy density before comparing to QCD. This is roughly equivalent to setting $T_{\mathcal{N}=4} = T_{\text{QCD}}/3^{1/4}$. The second part of the prescription is to determine $g_{YM}^2 N$ by

⁵Note from the discussion in the paragraph following (36) that a more accurate expression across a wide range of velocities is $\hat{q} = 2\pi\sqrt{g_{YM}^2 N} \frac{1}{v\sqrt{1-v^2}} T^3$. The difference between this form and the one in (43) is not significant for the purposes of the present discussion of highly relativistic quarks.

matching string theory results for the force between a static quark and anti-quark to lattice results. This match is conspicuously imperfect, but at $T_{\text{QCD}} = 250 \text{ MeV}$ a range $3.5 < g_{YM}^2 N < 8$ was found by comparing static potentials at $r \approx 0.25 \text{ fm}$, with $g_{YM}^2 N = 5.5$ suggested as a typical value. To summarize:

$$\text{"alternative" scheme: } \quad 3^{1/4} T_{\mathcal{N}=4} = T_{\text{QCD}} = 250 \text{ MeV} \quad g_{YM}^2 N = 5.5. \quad (45)$$

Combining (43) with either (44) and (45) leads to the following estimates of \hat{q} for charm quarks propagating through a real QGP:

$$\begin{aligned} \text{"obvious":} \quad \hat{q} &\approx (2.2 \text{ GeV}^2/\text{fm}) \frac{v}{\sqrt{1-v^2}} = 15 \text{ GeV}^2/\text{fm} & \text{for } p_c = 10 \text{ GeV}/c \\ \text{"alternative":} \quad \hat{q} &\approx (0.51 \text{ GeV}^2/\text{fm}) \frac{v}{\sqrt{1-v^2}} = 3.7 \text{ GeV}^2/\text{fm} & \text{for } p_c = 10 \text{ GeV}/c, \end{aligned} \quad (46)$$

where I have set $m_c = 1.4 \text{ GeV}$. The choice $p_c = 10 \text{ GeV}/c$ corresponds roughly to $p_T = 5 \text{ GeV}$ for non-photonic electrons.⁶ As will be explained in section 6.2, the rate of energy loss in the trailing string picture is not related to \hat{q} in the same way as it is in the treatment of [1]. Thus the values in (46) are more directly relevant to p_\perp broadening than to energy loss.

There appears to be some tension between the present work and [2]. We insert a color source in $\mathcal{N} = 4$ gauge theory in the same way, namely by letting a fundamental string end on the boundary. This is why our results have the same $\sqrt{g_{YM}^2 N}$ scaling. But the functional dependence as well as the magnitude of our results differ significantly: in [2] it was found that

$$\hat{q}_{\text{LRW}} = \frac{\pi^{3/2} \Gamma(3/4)}{\Gamma(5/4)} \sqrt{g_{YM}^2 N} T^3 \quad (47)$$

in the light-like limit, $v \rightarrow 1$. This corresponds as per (34) to $\hat{Q}_{\text{LRW}} = \sqrt{\pi} \Gamma(3/4) / 2 \Gamma(5/4) \approx 1.2$, which is roughly 3/5 times the minimal value of \hat{Q} found using (35): see figure 2. In [2], \hat{q} is calculated rather differently from the approach herein. In fact, not even the definition of \hat{q} is the same. It should also be recalled that I claim to be computing \hat{q} for heavy quarks, while the authors of [2] have argued that their results apply for light quarks. It is interesting to note that if a factor of $1/\sqrt{1-v^2}$ is dropped from (43), the result coincides in the $v \rightarrow 1$

⁶I thank B. Zajc for correspondence on this point and regarding the interesting p_T dependence of R_{AA} for non-photonic electrons as reported in [37].

limit to the naive extrapolation of the non-relativistic limit, $\hat{q} = 2\pi\sqrt{g_{YM}^2 N} T^3/v$.⁷ The value of this expression at $v = 1$ is about $0.83\hat{q}_{LRW}$. I do not know what meaning to attach to these numerical observations.

The trailing string makes the distinctive prediction that both the drag force and \hat{q} for a heavy quark are approximately proportional to the Lorentz factor $1/\sqrt{1-v^2}$ for v close to 1. This clearly implies that heavy quarks feel dissipative effects more strongly when they are more energetic. So the expectation from the trailing string picture is that R_{AA} as a function of p_T for non-photonic electrons has a more negative slope than predicted by treatments such as [39] in which \hat{q} is held fixed (i.e. independent of p_T). Thus it is gratifying to observe in figure 3 of [37] a persistently negative slope of R_{AA} over a wide range of momenta, $1.5 \text{ GeV}/c < p_T < 7 \text{ GeV}/c$. The predictions of [39] include a weaker dependence of R_{AA} on p_T over this range.⁸ It is tempting to draw some support for the trailing string picture of heavy energy loss from this comparison. But two caveats should be noted:

1. Only three or perhaps four data points in [37] lie below the predictions of [39]. These points have $p_T > 4 \text{ GeV}/c$. Only three points are below the range predicted by [40], in which energy loss is enhanced through interaction with D - and B -like resonances in the QGP.
2. The comparisons I have made to [39] are incomplete at best. A proper comparison to this work and to [37] would include a full calculation of quenching weights, which is beyond the scope of this paper.

Results from the STAR collaboration [36] agree fairly well with [39] if the contribution from bottom quarks is removed. But in light of the comparisons of $pp \rightarrow eX$ PHENIX data [41] with fixed-order-plus-next-to-leading-log calculations [42], it seems ad hoc to neglect bottom contributions completely. The authors of [39] cogently warn of the difficulty of disentangling the contributions of charm and bottom in the absence of vertex reconstruction. In any case, the STAR data are at least consistent with a more negative slope for R_{AA} as a function of p_T than either the $c+b$ or c only curves from [39].

⁷I thank K. Rajagopal for discussions on this point. Also note that the conjectured exact form $\hat{q} = 2\pi\sqrt{g_{YM}^2 N} \frac{1}{v\sqrt{1-v^2}} T^3$ is *exactly* $1/\sqrt{1-v^2}$ times the non-relativistic expression.

⁸In referring to the predictions of one or another theoretical study, I am relying upon the portrayal of those predictions in [37] or [36]. This means, in particular, a choice $\hat{q} = 14 \text{ GeV}^2/\text{fm}$ in the calculations of [39].

6.2 Energy loss and p_\perp broadening

An argument based on the uncertainty principle led the authors of [43] to the inequality

$$-\frac{dE}{dx^1} < \frac{1}{2}\hat{q}\lambda. \quad (48)$$

To be more precise, the inequality is $-\Delta E < \frac{1}{2}\hat{q}\lambda^2$ where ΔE is the energy loss (a negative quantity) for a parton traveling through a medium of thickness λ . Thus the left hand side of (48) is the average energy loss, $-\Delta E/\lambda$. The trailing string paradigm predicts both dE/dx^1 ,⁹

$$-\frac{dE}{dx^1} = -\frac{dp_1}{dt} = -F_{\text{drag}} = \frac{\pi\sqrt{g_{YM}^2 N}}{2} \frac{v}{\sqrt{1-v^2}} T^2, \quad (49)$$

and the jet-quenching parameter (evaluated at zero frequency),

$$\hat{q} = 2\pi\sqrt{g_{YM}^2 N} \hat{Q} T^3 > 2\pi\sqrt{g_{YM}^2 N} \frac{v}{\sqrt{1-v^2}} T^3, \quad (50)$$

where the inequality is nearly saturated when v is close to 1.¹⁰ Combining (49) and (50), one finds

$$-\frac{dE}{dx^1} = \frac{v/\hat{Q}}{\sqrt{1-v^2}} \frac{\hat{q}}{4T} < \frac{\hat{q}}{4T}. \quad (51)$$

The inequality in (51) implies (48) provided $\lambda > 1/2T$, which is a safe bet if λ is comparable to the system size and if thermalization actually occurs. If the hard parton traverses a distance λ smaller than $1/T$, the whole trailing string construction is highly suspect, because it relies on a late time limit.

Recalling that the inequality (51) is nearly saturated when v is close to 1, one sees that energy loss scales as λ rather than the familiar λ^2 that arises when $dE/dx^1 \propto \hat{q}\lambda$. Scaling of ΔE with λ^2 arises not only in the BDMPS approach [44, 1], but also in the complementary description of [45] when the energy of the quark is large enough. To consider this point in more detail, consider the energy loss formula

$$-\frac{dE}{dx^1} = \frac{1}{8}\hat{q}\lambda, \quad (52)$$

where the $1/8$ follows from choosing $\alpha_s = 1/3$ in (3.13) of [1]. As before, the left hand side is

⁹As noted in [3], the first inequality in (49) doesn't rely on $E = m/\sqrt{1-v^2}$ and $p = mv/\sqrt{1-v^2}$, but only on $dE/dp = v = dx^1/dt$.

¹⁰If \hat{q} is evaluated at a non-zero frequency, e.g. $\omega \sim 1/L$, it just gets bigger, so the inequality in (50) still holds.

really an averaged derivative, $-\Delta E/\lambda$. Setting ΔE equal to the initial energy E_0 one finds an approximate stopping length

$$\lambda_{\text{stop}} = \sqrt{\frac{8E}{\hat{q}}} = 1.3 \text{ fm} \sqrt{\frac{E/(10 \text{ GeV})}{\hat{q}/(10 \text{ GeV}^2/\text{fm})}}. \quad (53)$$

In contrast, the trailing string picture predicts a relaxation time t_D for heavy quarks that is independent of their energy (up to issues related to dispersion relations as discussed in [3]). Estimates of t_D for charm range from 0.6 fm in the “obvious” scheme to 2.1 fm in the “alternative” scheme (for a summary, see [38]).

As a final comparison between trailing string predictions and a more conventional treatment based on (52), consider the relative strength of stopping versus turning effects by defining a turning length

$$\lambda_{\text{turn}} = p_0^2/\hat{q} \quad (54)$$

for a parton of initial momentum p_0 . If energy loss is ignored, then the rms transverse momentum becomes equal to p_0 after the parton traverses a path length λ_{turn} . For a stopping length I will use λ_{stop} of (53) in the BDMPS approach. In string theory I will use

$$\lambda_{\text{stop}} = vt_D = \frac{2v}{\pi\sqrt{g_{YM}^2 N}} \frac{m}{T^2}, \quad (55)$$

and of course (54) still applies, for the appropriate stringy \hat{q} . In the limit of highly relativistic partons one may straightforwardly evaluate the ratios

$$\begin{aligned} \text{BDMPS @ } \hat{q} = 14 \text{ GeV}^2/\text{fm:} \quad & \frac{\lambda_{\text{turn}}}{\lambda_{\text{stop}}} \approx \sqrt{\frac{E_0^3}{8\hat{q}}} \approx \left(\frac{E_0}{2.8 \text{ GeV}}\right)^{3/2} \\ \text{trailing string @ } T = 250 \text{ MeV:} \quad & \frac{\lambda_{\text{turn}}}{\lambda_{\text{stop}}} \approx \frac{E_0}{4T} = \frac{E_0}{1 \text{ GeV}}. \end{aligned} \quad (56)$$

The differing power laws are another manifestation of the different scaling of energy loss with path length. In the trailing string case, the large value of $\lambda_{\text{turn}}/\lambda_{\text{stop}}$ is reassuring because it says that the classical drag force is stronger than the fluctuation effects that cause diffusion of the transverse momentum—provided one avoids the limit of small velocity, where it is probably better to think of diffusion of three-dimensional momentum.

Although energy loss and p_\perp broadening are clearly linked in the trailing string picture, as they are in the BDMPS approach, the differing relative strengths of these effects, as crudely summarized in (56), add to the motivation for finding a way of independently measuring the

two effects for heavy quarks.

Note added

After this work was completed, I received [46], which extends the results of [2, 34].

Acknowledgments

I thank C. Nayak, J. Maldacena, G. Michalogiorgakis, and B. Zajc for useful discussions. I am indebted to J. Friess, G. Michalogiorgakis, and S. Pufu for collaboration on work that led to the results appearing in appendix A. This work was supported in part by the Department of Energy under Grant No. DE-FG02-91ER40671, and by the Sloan Foundation.

A Infalling and outgoing coordinates

A crucial property of the wave-functions $\Psi(\omega, t, y)$ appearing in (14) is that they depend only on the infalling coordinate close to the horizon. The purpose of this appendix is to demonstrate that the infalling and outgoing coordinates are quoted correctly in (19), to leading order in small $y_S - y$, where as usual $y_S = \sqrt[4]{1 - v^2}$. Actually, I will do somewhat more by explicitly constructing coordinates in which the worldsheet metric is seen to be locally conformal to $\mathbf{R}^{1,1}$ (as any two-dimensional metric with $-+$ signature must be).

It is convenient to start by parametrizing the worldsheet using x^1 and y rather than t and y . The worldsheet metric is easily seen to be

$$ds_2^2 = g_{\alpha\beta} d\sigma^\alpha d\sigma^\beta = \frac{L^2}{z_H^2 y^2} \left[\left(1 - \frac{h}{v^2}\right) (dx^1)^2 - \frac{2z_H y^2}{v} dx^1 dy + z_H^2 dy^2 \right], \quad (57)$$

where as usual $h = 1 - y^4$. The manipulations to cast the metric (57) in a conformally flat form are relatively simple because $g_{\alpha\beta}$ depends on y but not x^1 :

$$\begin{aligned} ds_2^2 &= \frac{L^2}{y^2} \left(1 - \frac{y^4/v^2}{1 - h/v^2}\right) dy^2 + \frac{L^2}{z_H^2 y^2} \left(1 - \frac{h}{v^2}\right) \left(dx^1 - \frac{z_H y^2/v}{1 - h/v^2} dy\right)^2 \\ &= \frac{L^2}{y^2} \frac{1 - v^2}{h - v^2} dy^2 - \frac{L^2}{v^2 z_H^2 y^2} (h - v^2) dq^2 \\ &= \Omega^2 (-dq^2 + d\eta^2) \end{aligned} \quad (58)$$

where

$$\Omega^2 = \frac{L^2}{y^2} \frac{h - v^2}{v^2 z_H^2} \quad (59)$$

and I have defined new coordinates

$$q = x^1 + \int dy \frac{z_H y^2 v}{h - v^2} \quad \eta = \pm v z_H \sqrt{1 - v^2} \int \frac{dy}{h - v^2}. \quad (60)$$

Because $h - v^2 = y_S^4 - y^4$, the integrals in (60) diverge at the horizon. So one must define q and η piecewise in two regions:

$$\left. \begin{aligned} q_{\mathbf{I}} &= x^1 + \frac{z_H v}{4iy_S} \left(\log \frac{1 - iy/y_S}{1 + iy/y_S} + i \log \frac{1 + y/y_S}{1 - y/y_S} \right) \\ \eta_{\mathbf{I}} &= \frac{z_H v}{4iy_S} \left(-\log \frac{1 - iy/y_S}{1 + iy/y_S} + i \log \frac{1 + y/y_S}{1 - y/y_S} \right) \end{aligned} \right\} \quad \text{for } 0 < y < y_S; \quad (61)$$

$$\left. \begin{aligned} q_{\text{III}} &= x^1 + \frac{z_H v}{4i y_S} \left(\log \frac{1 - iy/y_S}{1 + iy/y_S} + i \log \frac{1 + y/y_S}{-1 + y/y_S} \right) \\ \eta_{\text{III}} &= \frac{z_H v}{4i y_S} \left(\log \frac{1 - iy/y_S}{1 + iy/y_S} - i \log \frac{1 + y/y_S}{-1 + y/y_S} \right) \end{aligned} \right\} \quad \text{for } y_S < y < 1, \quad (62)$$

The second form of the metric in (58) is analogous to the standard form of the Schwarzschild metric. In region **I** (outside the horizon) y is the spacelike variable and q is the timelike variable. In region **II** (inside the horizon) y is timelike and q is spacelike.

Using $x^1 = vt + \xi(y)$, one may extract expressions for q_{I} in terms of t and y rather than x^1 and y ; η_{I} , on the other hand, is a function only of y . To construct infalling and outgoing coordinates in region **I**, one simply forms

$$q_{\pm} = q_{\text{I}} \pm \eta_{\text{I}}. \quad (63)$$

Expanding in small $y_S - y$, one finds

$$q_- = vt + \dots \quad q_+ = v \left[t - \frac{z_H}{2y_S} \log(y_S - y) \right] + \dots, \quad (64)$$

where the omitted terms comprise constant terms (i.e. independent of t and y) and terms involving positive powers of $y_S - y$. Up to the overall factor of v , the expressions in (64) are precisely the ones given in (19).

B Speed limits on single quarks

The string theory calculations presented in this paper pertain to external quarks: pointlike objects in the fundamental representation which have infinite mass associated with their near-field Coulombic color-electric flux. Comparisons with QCD are thus better justified for c and b quarks, whose mass is well above the temperature, than for light quarks.

If the velocity of an external quark is too close to unity, there is a new reason to be wary of trailing string computations: the horizon on the worldsheet is very close to the boundary, where in a holographic representation of real QCD (assuming there is one) space presumably becomes highly curved, and the simplest calculations based on the Nambu-Goto action in AdS_5 -Schwarzschild-based may experience significant corrections. Let's try to estimate when problems of this sort might start to arise. It was suggested already in [22] to associate an energy scale

$$\mu = \frac{L^2/z_H}{2\pi\alpha'} \frac{1}{y} = \frac{T}{2} \frac{\sqrt{g_{YM}^2 N}}{y} \quad (65)$$

with a radius y in AdS_5 -Schwarzschild. This is justified by observing that a static string dangling from y into the horizon has mass

$$m_{\text{static}} = \frac{L^2/z_H}{2\pi\alpha'} \left(\frac{1}{y} - 1 \right) \approx \mu \quad \text{for } y \ll 1. \quad (66)$$

Now suppose one identifies a scale μ_{fail} at which AdS/CFT techniques (at least those based on supergravity and classical strings) start to fail. From (65) one extracts a corresponding y_{fail} , and if the worldsheet horizon has $y_S < y_{\text{fail}}$ there may be significant corrections to the trailing string results. Setting $y_S = y_{\text{fail}}$ and using (12), one finds that the Lorentz factor of the heavy quark that the trailing string purports to describe is

$$\gamma_{\text{fail}} = \frac{4}{g_{YM}^2 N} \left(\frac{\mu_{\text{fail}}}{T} \right)^2. \quad (67)$$

The trouble with (67) is that $g_{YM}^2 N$, μ_{fail} and T all incorporate considerable uncertainties.

To get an idea of the range of plausible values for γ_{fail} , let's consider the two prescriptions (44) and (45). I don't have a systematic way of determining μ_{fail} , but perhaps a reasonable range to consider is $\mu_{\text{fail}} = 0.8 - 1.6 \text{ GeV}$. Taking $\mu_{\text{fail}} = 1.2 \text{ GeV}$ as a representative value, one finds

$$\begin{aligned} \text{“obvious:”} \quad \gamma_{\text{fail}} &= 4.9 \left(\frac{\mu_{\text{fail}}}{1.2 \text{ GeV}} \right)^2 \\ \text{“alternative:”} \quad \gamma_{\text{fail}} &= 29 \left(\frac{\mu_{\text{fail}}}{1.2 \text{ GeV}} \right)^2. \end{aligned} \quad (68)$$

Because of the quadratic dependence on both μ_{fail} and T (not to mention the choice of comparison scheme) γ_{fail} remains substantially uncertain. Evidently, if the “obvious” prescription is used, there is some doubt cast on stringy predictions for charm quark when $p_c \gtrsim 6.7 \text{ GeV}/c$, corresponding to $p_T \gtrsim 3.4 \text{ GeV}$. In the “alternative” scheme, there is less reason to worry about stringy corrections near the upper end of the trailing string.

Another thing can go wrong if one wants to represent a finite mass quark as a string ending on a D7-brane, as in [47, 3]. Given m_c for the charm quark, one can use (66) to obtain a corresponding position

$$y_c = \frac{1}{1 + 2m_c/T \sqrt{g_{YM}^2 N}} \quad (69)$$

of the D7-brane. If $y_S < y_c$, then there is no horizon on the trailing string: the boundary of the worldsheet is spacelike. I regard this as a pathology which probably invalidates the trailing string picture for Lorentz factors $\gamma > \gamma_c \equiv 1/y_c^2$. Estimates of γ_c suffer from the

same ambiguities as γ_{fail} , as discussed above. Using $m_c = 1.4 \text{ GeV}$ and either (44) or (45), one arrives at the estimates

$$\begin{array}{ll} \text{“obvious:”} & \gamma_c = 13 \\ \text{“alternative:”} & \gamma_c = 53. \end{array} \quad (70)$$

These values should again be regarded as incorporating considerable uncertainties: for example, it is puzzling that the horizon causes the mass of a quark to *decrease* from its zero-temperature value, but this decrease is what makes the values in (70) higher than those derived from (68) with $\mu_{\text{fail}} \rightarrow m_c$. The main lesson to draw from (70) is that charm’s mass is high enough to avoid threatening the existence of the worldsheet horizon for the momenta accessible at RHIC; but attempts to treat light quarks in terms of the trailing string construction are perilous indeed.¹¹

¹¹For example, in the “alternative” comparison scheme, an up quark whose mass in the medium is assumed to be $m = 300 \text{ MeV}$ would be described in terms of a D7-brane with $y_u = 0.43$, so $\gamma_u = 5.5$ is the maximum Lorentz factor. It is hardly fair to ignore corrections to relativistic dispersion relations in this context, but if one does so, the result is a total energy of 1.7 GeV . As an upper limit on allowed energies for partons described by trailing strings, this is pretty anemic.

References

- [1] R. Baier, Y. L. Dokshitzer, A. H. Mueller, S. Peigne, and D. Schiff, “Radiative energy loss and $p(T)$ -broadening of high energy partons in nuclei,” *Nucl. Phys.* **B484** (1997) 265–282, [hep-ph/9608322](#).
- [2] H. Liu, K. Rajagopal, and U. A. Wiedemann, “Calculating the jet quenching parameter from AdS/CFT,” [hep-ph/0605178](#).
- [3] C. P. Herzog, A. Karch, P. Kovtun, C. Kozcaz, and L. G. Yaffe, “Energy loss of a heavy quark moving through $N = 4$ supersymmetric Yang-Mills plasma,” [hep-th/0605158](#).
- [4] J. Casalderrey-Solana and D. Teaney, “Heavy quark diffusion in strongly coupled $N = 4$ Yang Mills,” [hep-ph/0605199](#).
- [5] S. S. Gubser, “Drag force in AdS/CFT,” [hep-th/0605182](#).
- [6] S.-J. Sin and I. Zahed, “Holography of radiation and jet quenching,” *Phys. Lett.* **B608** (2005) 265–273, [hep-th/0407215](#).
- [7] A. Buchel, “On jet quenching parameters in strongly coupled non-conformal gauge theories,” *Phys. Rev.* **D74** (2006) 046006, [hep-th/0605178](#).
- [8] E. Nakano, S. Teraguchi, and W.-Y. Wen, “Drag force, jet quenching, and AdS/QCD,” [hep-ph/0608274](#).
- [9] P. Talavera, “Drag force in a string model dual to large- N QCD,” [hep-th/0610179](#).
- [10] Y.-h. Gao, W.-s. Xu, and D.-f. Zeng, “Jet quenching parameters of Sakai-Sugimoto model,” [hep-th/0611217](#).
- [11] C. P. Herzog, “Energy loss of heavy quarks from asymptotically AdS geometries,” *JHEP* **09** (2006) 032, [hep-th/0605191](#).
- [12] E. Caceres and A. Guijosa, “Drag force in charged $N = 4$ SYM plasma,” *JHEP* **11** (2006) 077, [hep-th/0605235](#).
- [13] F.-L. Lin and T. Matsuo, “Jet quenching parameter in medium with chemical potential from AdS/CFT,” *Phys. Lett.* **B641** (2006) 45–49, [hep-th/0606136](#).

- [14] S. D. Avramis and K. Sfetsos, “Supergravity and the jet quenching parameter in the presence of R-charge densities,” [hep-th/0606190](#).
- [15] N. Armesto, J. D. Edelstein, and J. Mas, “Jet quenching at finite ’t Hooft coupling and chemical potential from AdS/CFT,” *JHEP* **09** (2006) 039, [hep-ph/0606245](#).
- [16] E. Caceres and A. Guijosa, “On drag forces and jet quenching in strongly coupled plasmas,” [hep-th/0606134](#).
- [17] J. F. Vazquez-Poritz, “Enhancing the jet quenching parameter from marginal deformations,” [hep-th/0605296](#).
- [18] J. J. Friess, S. S. Gubser, and G. Michalogiorgakis, “Dissipation from a heavy quark moving through $N = 4$ super-Yang-Mills plasma,” *JHEP* **09** (2006) 072, [hep-th/0605292](#).
- [19] J. J. Friess, S. S. Gubser, G. Michalogiorgakis, and S. S. Pufu, “The stress tensor of a quark moving through $N = 4$ thermal plasma,” [hep-th/0607022](#).
- [20] S.-J. Sin and I. Zahed, “Ampere’s law and energy loss in AdS/CFT duality,” [hep-ph/0606049](#).
- [21] M. Chernicoff and A. Guijosa, “Energy loss of gluons, baryons and k-quarks in an $N = 4$ SYM plasma,” [hep-th/0611155](#).
- [22] J. M. Maldacena, “The large N limit of superconformal field theories and supergravity,” *Adv. Theor. Math. Phys.* **2** (1998) 231–252, [hep-th/9711200](#).
- [23] S. S. Gubser, I. R. Klebanov, and A. M. Polyakov, “Gauge theory correlators from non-critical string theory,” *Phys. Lett.* **B428** (1998) 105–114, [hep-th/9802109](#).
- [24] E. Witten, “Anti-de Sitter space and holography,” *Adv. Theor. Math. Phys.* **2** (1998) 253–291, [hep-th/9802150](#).
- [25] O. Aharony, S. S. Gubser, J. M. Maldacena, H. Ooguri, and Y. Oz, “Large N field theories, string theory and gravity,” *Phys. Rept.* **323** (2000) 183–386, [hep-th/9905111](#).
- [26] E. D’Hoker and D. Z. Freedman, “Supersymmetric gauge theories and the AdS/CFT correspondence,” [hep-th/0201253](#).

- [27] I. R. Klebanov, “TASI lectures: Introduction to the AdS/CFT correspondence,” [hep-th/0009139](#).
- [28] S.-J. Rey and J.-T. Yee, “Macroscopic strings as heavy quarks in large N gauge theory and anti-de Sitter supergravity,” *Eur. Phys. J.* **C22** (2001) 379–394, [hep-th/9803001](#).
- [29] J. M. Maldacena, “Wilson loops in large N field theories,” *Phys. Rev. Lett.* **80** (1998) 4859–4862, [hep-th/9803002](#).
- [30] D. T. Son and A. O. Starinets, “Minkowski-space correlators in AdS/CFT correspondence: Recipe and applications,” *JHEP* **09** (2002) 042, [hep-th/0205051](#).
- [31] S. S. Gubser, I. R. Klebanov, and A. W. Peet, “Entropy and Temperature of Black 3-Branes,” *Phys. Rev.* **D54** (1996) 3915–3919, [hep-th/9602135](#).
- [32] A. E. Lawrence and E. J. Martinec, “Black hole evaporation along macroscopic strings,” *Phys. Rev.* **D50** (1994) 2680–2691, [hep-th/9312127](#).
- [33] K. Peeters, J. Sonnenschein, and M. Zamaklar, “Holographic melting and related properties of mesons in a quark gluon plasma,” *Phys. Rev.* **D74** (2006) 106008, [hep-th/0606195](#).
- [34] H. Liu, K. Rajagopal, and U. A. Wiedemann, “An AdS/CFT calculation of screening in a hot wind,” [hep-ph/0607062](#).
- [35] M. Chernicoff, J. A. Garcia, and A. Guijosa, “The energy of a moving quark-antiquark pair in an $N = 4$ SYM plasma,” *JHEP* **09** (2006) 068, [hep-th/0607089](#).
- [36] **STAR** Collaboration, B. I. Abelev *et. al.*, “Transverse momentum and centrality dependence of high- $p(T)$ non-photonic electron suppression in Au + Au collisions at $\sqrt{s_{NN}} = 200$ GeV,” [nucl-ex/0607012](#).
- [37] **PHENIX** Collaboration, A. Adare *et. al.*, “Energy Loss and Flow of Heavy Quarks in Au+Au Collisions at $\sqrt{s_{NN}} = 200$ GeV,” [nucl-ex/0611018](#).
- [38] S. S. Gubser, “Comparing the drag force on heavy quarks in $N = 4$ super-Yang-Mills theory and QCD,” [hep-th/0611272](#).
- [39] N. Armesto, M. Cacciari, A. Dainese, C. A. Salgado, and U. A. Wiedemann, “How sensitive are high- $p(T)$ electron spectra at RHIC to heavy quark energy loss?,” *Phys. Lett.* **B637** (2006) 362–366, [hep-ph/0511257](#).

- [40] R. Rapp and H. van Hees, “Heavy-quark diffusion, flow and recombination at RHIC,” [hep-ph/0606117](#).
- [41] **PHENIX** Collaboration, A. Adare *et. al.*, “Measurement of high-p(T) single electrons from heavy-flavor decays in p + p collisions at $\sqrt{s} = 200$ GeV,” [hep-ex/0609010](#).
- [42] M. Cacciari, P. Nason, and R. Vogt, “QCD predictions for charm and bottom production at RHIC,” *Phys. Rev. Lett.* **95** (2005) 122001, [hep-ph/0502203](#).
- [43] S. J. Brodsky and P. Hoyer, “A Bound on the energy loss of partons in nuclei,” *Phys. Lett.* **B298** (1993) 165–170, [hep-ph/9210262](#).
- [44] R. Baier, Y. L. Dokshitzer, A. H. Mueller, S. Peigne, and D. Schiff, “Radiative energy loss of high energy quarks and gluons in a finite-volume quark-gluon plasma,” *Nucl. Phys.* **B483** (1997) 291–320, [hep-ph/9607355](#).
- [45] B. G. Zakharov, “Radiative energy loss of high energy quarks in finite-size nuclear matter and quark-gluon plasma,” *JETP Lett.* **65** (1997) 615–620, [hep-ph/9704255](#).
- [46] H. Liu, K. Rajagopal, and U. A. Wiedemann, “Wilson loops in heavy ion collisions and their calculation in AdS/CFT,” [hep-ph/0612168](#).
- [47] A. Karch and E. Katz, “Adding flavor to AdS/CFT,” *JHEP* **06** (2002) 043, [hep-th/0205236](#).